Sterically Stabilized Colloids with Tunable Repulsions

ARTICLE *in* LANGMUIR · AUGUST 2013

Impact Factor: 4.46 · DOI: 10.1021/la402104q · Source: PubMed

5 AUTHORS, INCLUDING:

Kitty van Gruijthuijsen
Firmenich
11 PUBLICATIONS **45** CITATIONS
SEE PROFILE

Marc Obiols-Rabasa
Lund University
17 PUBLICATIONS **59** CITATIONS
SEE PROFILE

Marco Heinen
California Institute of Technology
22 PUBLICATIONS **201** CITATIONS
SEE PROFILE

Langmuir

Article

pubs.acs.org/Langmuir

Sterically Stabilized Colloids with Tunable Repulsions

Kitty van Gruijthuijsen,[†] Marc Obiols-Rabasa,[‡] Marco Heinen,[§] Gerhard Nägele,[∥] and Anna Stradner*[,‡]

[†]Adolphe Merkle Institute, University of Fribourg, Rte de l'ancienne Papeterie 1, CH-1723 Marly, Switzerland

[‡]Physical Chemistry, Lund University, Getingevägen 60, SE-221 00 Lund, Sweden

[§]Institut für Theoretische Physik II - Soft Matter, Heinrich-Heine-Universität Düsseldorf, D-40225 Düsseldorf, Germany

[∥]Institute of Complex Systems (ICS-3), Forschungszentrum Jülich, D-52425 Jülich, Germany

Supporting Information

ABSTRACT: When studying tunable electrostatic repulsions in aqueous suspensions of charged colloids, irreversible colloid aggregation or gelation may occur at high salt concentrations. For many commonly used synthetic colloids, such as polystyrene and silica particles, the reason for coagulation is the presence of unbalanced, strongly attractive, and short-ranged van der Waals (VDW) forces. Here, we present an aqueous polystyrene model colloid that is sterically stabilized against VDW attractions. We show that the synthesis procedure, based on a neutral initiator couple and a nonionic surfactant, introduces surface charges that can be further increased by the addition of charged comonomer methacrylic acid. Thus, the interactions between the polystyrene spheres can be conveniently tuned from hard-sphere-like to charge-stabilized with long-ranged electrostatic repulsions described by a Yukawa-type pair potential. The particle size, grafting density, core−shell structure, and surface charge are characterized by light and neutron scattering. Using X-ray and neutron scattering in combination with an accurate analytic integral equation scheme for the colloidal static structure factor, we deduce effective particle charges for colloid volume fractions ≥0.1 and salt concentrations in the range of 1.5 to 50 mM.

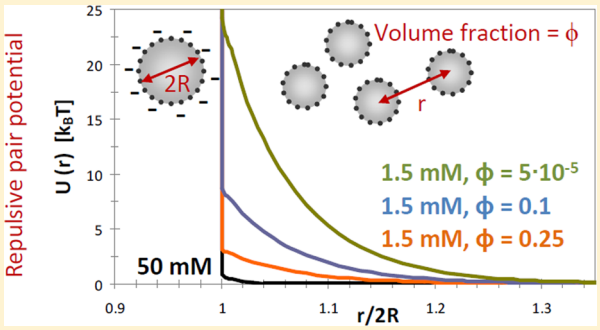

INTRODUCTION

Practically all colloids carry surface charges when dispersed in water.[1] These charges can originate from intrinsically charged surface groups, such as acids or bases, or result from ion adsorption from the solvent. Electrostatic repulsions between colloids can be used to stabilize dispersions against attractions[1−4] and to create highly ordered structures that show optical effects such as Bragg reflections and optical band gaps.[5−7] To tune the properties of charged systems, it is crucial to understand and to be able to describe the repulsive colloidal interactions over a wide range of dispersion properties.[8] However, a proper experimental characterization of the effect of surface charges, including the limit of vanishing electrostatic repulsions, is often hampered by the presence of van der Waals (VDW) attractions in aqueous suspensions of model colloidal particles such as polystyrene (PS) and silica spheres.[3,9]

In a typical Derjaguin−Landau−Verwey−Overbeek (DLVO)-type description of the stability of charged colloids,[10,11] screening of the charges by the addition of salt induces an interplay between the repulsions and VDW attractions.[2,3,12,13] The strength of the repulsions is determined by the number of effective surface charges, Z_{eff}, and the range is determined by the Debye length, κ^{-1}, which is inversely proportional to the square root of the salt concentration for higher salt content. The strength of the VDW attractions is largely determined by the difference in the refractive indices of the solvent and the colloids.[14,15] It can therefore be minimized by choosing a (nearly) refractive index matching solvent, such as a mixture of toluene and ethanol to match silica colloids.[16−18] However, in aqueous colloidal suspensions, in which relevant properties such as salt solubility and dielectric permittivity are markedly higher than in organic solvents, refractive index matching would require a cumbersome synthesis of fluorinated colloids.[19] Another elegant way to minimize the effects of the VDW attractions is to coat the colloids with a layer of soluble polymer.[20] The swollen polymer chains prevent two colloids from approaching close enough for the attractions to cause aggregation. A sufficiently dense polymer layer that extends far enough into the solution thus creates steric stabilization of the colloids. In this way, one can exclusively study the effect of electrostatic repulsions by the variation of the salt concentration.

In this article, we define an aqueous colloidal model system that is fully stabilized against VDW attractions and exhibits tunable screened Coulomb repulsions. Although such systems have been reported before,[21−23] a thorough characterization of the repulsions at higher colloid concentrations is often lacking. A well-defined system can be used to address fundamental questions about colloids interacting via screened Coulomb

Received: December 16, 2012
Published: August 12, 2013

   dx.doi.org/10.1021/la402104q | Langmuir 2013, 29, 11199−11207

repulsions with respect to fluid−crystal coexistence,[24] glassy states, or in combination with polymer-induced depletion attractions.[25] We adapt the synthesis reported by Weiss and coworkers for polystyrene colloids that are sterically stabilized by the commercial surfactant Tween 80[26] by adding methacrylic acid as a comonomer to introduce surface charges.[27] We systematically characterize the internal core−shell structure of the colloids as well as the ionic-strength- and concentration-dependent equilibrium microstructure of aqueous suspensions using both small-angle neutron and X-ray scattering (SANS and SAXS)[23] in combination with a numerically efficient semi-analytic integral equation scheme for the static pair-correlation function, referred to as the modified penetrating background corrected rescaled mean spherical approximation (MPB-RMSA).[17]

EXPERIMENTAL SECTION

Materials. Styrene (Fluka, ≥99%) was purified over a column of aluminum oxide (Merck). Poly(ethylene glycol) sorbitan monooleate (Tween 80, functionality 0.7, Sigma-Aldrich), ascorbic acid (Fluka), H_2O_2 (35%, Fluka), methacrylic acid (Sigma-Aldrich), sodium chloride (Reactolab), and sodium azide (AppliChem) were used without further purification. Solvent D_2O was purchased from Cambridge Isotope Laboratories, and partially deuterated styrene ($C_8H_3D_5$, >98%) was purchased from Polymer Source.

Emulsion Polymerization. Polystyrene (PS) spheres were prepared by emulsion polymerization in a batch reactor.[26,28] Typically, a 500 mL round-bottomed flask was charged with 220 mL of water, 10 g of styrene, and 1.4 g of Tween 80 (Figure 1). The mixture was

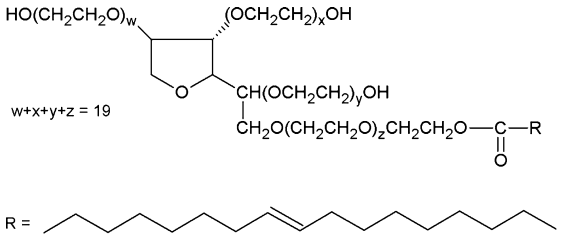

Figure 1. Structure of Tween 80.

placed in a nitrogen atmosphere, heated to 60 °C, and magnetically stirred at 550 min^{-1}. The reaction was started by the addition of neutral initiator couple ascorbic acid and H_2O_2 and was allowed to go to completion over 22 h. Anionic comonomer methacrylic acid was introduced 30 min after initialization. The compositions of different reaction mixtures are shown in Table 1, with NI referring to nonionic synthesis and MA referring to the presence of methacrylic acid. Coagulum was removed by four consecutive filtering steps over a folded filter and over 5, 1.2, and 0.45 μm PVDF filter membranes (Millipore). The colloidal suspension was cleaned by diafiltration with deionized water (Sartorius) over a 300 kDa filter (Biomax, Millipore). The final ionic strength was set by diafiltration with a 3 mM NaN_3 solution to prevent microbial growth.

Table 1. Composition of the Synthesis Mixtures[a]

colloid batch	mmol H_2O_2/ mol styrene	g Tween 80/ g styrene	mmol comonomer/ mol styrene
NI1	7	0.14	
NI2	10	0.15	
MA1	7	0.14	0.14
MA2	8	0.14	3.3
MA3	9	0.14	3.3

[a]For colloid batch NI2, partly deuterated styrene was used. The nonionic initiator couple consisted of H_2O_2, with amounts as listed, and ascorbic acid, which functions as a catalyzer and was added in a three-fold-lower quantity.

Colloid batches MA2 and MA3 were further concentrated by gravitational filtration lasting 2 days to final mass concentrations of c = 396 and 440 g/L, respectively, as determined with a moisture analyzer (MA35, Sartorius). All dilutions of the colloid stock solutions were prepared with stock solutions of NaCl. The final salt concentrations in the continuous aqueous phase that are reported throughout this article are the total NaN_3 present from the stock solution and NaCl used in the dilution media, with both being 1:1 salts.

Dynamic Light Scattering. Dynamic light scattering measurements were performed at an angle of $\theta = 90°$ on a 3D LS spectrometer (LS Instruments) equipped with a HeNe laser operating at a wavelength of λ = 632.8 nm. The colloids were diluted in H_2O to a final concentration of c = 0.05 g/L and filtered prior to the measurements (Millipore syringe filters, 220 nm pore size). The average hydrodynamic radius, R_h, of the colloids and their size polydispersity (i.e., the standard deviation in R_h) were extracted using the cumulant method.[29,30]

Zeta Potential. The electrophoretic mobility, μ_e, of uncorrelated colloids in highly diluted suspensions was determined using the Zetasizer Nano (Malvern Instruments). For this purpose, colloid stock solutions were diluted to c = 0.05 g/L in NaCl/NaN_3 solutions of c_s = 0.2, 0.5, 1, 2, 5, 10, and 20 mM and filtered prior to the measurements (Millipore syringe filters, 220 nm pore size). The zeta potential, ζ, was estimated from the measured μ_e data employing the linear Henry formula (in SI units)

$$\zeta = \frac{\mu_e \eta}{\varepsilon\varepsilon_0 f(\kappa_s R_h)} \tag{1}$$

where η = 0.93 mPa·s is the viscosity of water at 22 °C and $\varepsilon\varepsilon_0 = 7.08 \times 10^{-10}$ $C^2 \cdot s^2 \cdot kg^{-1} \cdot m^{-3}$ is the permittivity of water. The Henry function $f(\kappa_s R_h)$ is well approximated by Ohshima's expression:[31]

$$f(\kappa_s R_h) = \frac{2}{3}\left[1 + \frac{1}{2}\left(1 + \frac{2.5}{\kappa_s R_h (1 + 2\exp(-\kappa_s R_h))}\right)^{-3}\right] \tag{2}$$

Because the zeta potential is determined in the plane of zero shear, R_h values from DLS are used for the colloid radius. Under the low colloid concentration and relatively high salinity conditions in the electrophoretic experiments, the concentration of counterions released from the colloid surface is negligible, and the inverse Debye length, κ_s, for 1:1 salts is given by $\kappa_s = (8\pi c_s N_A l_B)^{1/2}$. Here, $l_B = z_e^2/4\pi\varepsilon\varepsilon_0 k_B T \approx 7 \times 10^{-10}$ m is the Bjerrum length in water at room temperature, N_A is Avogadro's number, z_e is the positive elementary charge, k_B is Boltzmann's constant, and T is the absolute temperature.

To obtain an estimate of the electrophoretic effective charge, Z_{ep}, the zeta potential is assumed to be equal to the surface potential. A linear relation between Z_{ep} and ζ is used, consistent with eq 1 and in line with a similar approximate treatment by Palberg and coworkers:[32,33]

$$Z_{ep} = \frac{\zeta}{z_e}(4\pi\varepsilon\varepsilon_0 R_h (1 + \kappa_s R_h)) \tag{3}$$

We have verified that interparticle correlations are negligible under the electrophoretic measurement conditions.

Small-Angle Neutron and X-ray Scattering. The internal structure of the core−shell colloids was studied with small-angle neutron scattering on the SANS-I instrument at the Paul Scherrer Institute, Villigen, Switzerland. Partially deuterated colloids (NI2) were prepared in a series of H_2O/D_2O mixtures with 10 mM NaCl/NaN_3 and measured in 2 mm quartz cells (120-QS, Hellma) for D_2O contents >50% or in 1 mm quartz cells (120-QS, Hellma) for D_2O contents <50%. A beam of neutrons with λ = 0.8 nm (10% wavelength spread) was collimated over 18 m, and scattered neutrons were collected at a sample−detector distance of 18 m. Scattering intensities were corrected for the detector efficiency and scaled to absolute differential scattering cross sections, $d\Sigma(q)/d\Omega$, using a water

dx.doi.org/10.1021/la402104q | Langmuir 2013, 29, 11199−11207

measurement at a 4.5 m sample−detector distance and a 4.5 m collimation.[34] The covered q range was 0.025−0.3 nm^{-1}, where q is the scattering wavenumber related to the scattering angle θ and incident radiation wavelength λ by $q = 4\pi \sin(\theta/2)/\lambda$.[35]

SANS-I was also used to study the structuring of charged colloids (MA3) at higher concentrations but now with λ = 1.2 nm neutrons, which were focused onto the sample with 11 neutron lenses, yielding highly resolved scattering patterns at a sample−detector distance of 20 m. Scattering intensities were corrected for detector efficiency and brought to absolute scale in the same way as described above.[34] The same samples (MA3) and concentration series of colloid batch MA2 were measured with small-angle X-ray scattering (SAXS). These experiments were performed on the coherent SAXS (cSAXS) instrument at the Paul Scherrer Institute (Villigen, Switzerland), with 11.2 eV X-rays corresponding to λ = 0.111 nm. The covered q ranges were 0.009−0.2 nm^{-1} with SANS-I and 0.009−1 nm^{-1} with cSAXS. SANS measurements were performed in 1 mm quartz cells (120-QS, Hellma), and cSAXS measurements were performed in 1 mm glass mark tubes (Hilgenberg).

RESULTS AND DISCUSSION

Steric Stabilization. A grafted polymeric shell is an efficient means to stabilize colloids against VDW attractions but introduces an inherent degree of softness onto the colloids as a result of the hairy nature of the polymers in the shell. Discrepancies between theoretical work on hard spheres and experimental results of effective hard spheres are often related to this softness, especially in the limit of closely packed colloids in crystals, glasses, and gels.[24] To quantify its effect, it is important to know the average grafting density and the thickness of the polymeric shell.

To determine these parameters, we used partially deuterated styrene, $C_8H_3D_5$, as a monomer in the synthesis of NI2, which allowed us to perform a contrast variation study with small-angle neutron scattering (SANS).[22,28] The neutron scattering length densities of the partially deuterated polystyrene core, δ_c, and that of the Tween 80 shell, δ_s, are in between the neutron scattering length densities of H_2O and D_2O while significantly differing from each other. Thus, it is possible to vary the separate scattering contributions from the core and the shell by the variation of the H_2O/D_2O mixing ratio.

The scattering curves for colloid batch NI2 under different contrast conditions (i.e., in H_2O/D_2O mixtures with different mixing ratios) are shown in Figure 2 as symbols. As anticipated, the shape and absolute height of the curves are strongly affected by the solvent composition. To model the data, we adapted an analytical model with which we previously successfully described the scattering from core−shell particles with a larger poly(ethylene glycol) (PEG) shell.[28] The radial profile of the scattering length density that best describes the measured curves is depicted in the inset of Figure 2A. A detailed description of the model parameters is given in the Supporting Information. The strength of the analytical form factor model is that each of the five independent fitting parameters, used to fit the eight scattering curves in Figure 2, is a distinct physical quantity representing the chemical composition of the core and the shell independently of the solvent composition. Within these model constraints, the agreement between the model calculations (solid lines) and the SANS curves (symbols) at eight different H_2O/D_2O ratios is quite good.

We find a core radius of R_c = 45 nm with a size polydispersity of s = 0.08 and a number of grafted chains per colloid of N_{agg} = 15 700. From R_c and N_{agg}, the grafting density of the surfactant is derived to be Σ_s = 0.62 nm^{-2}. The molecular area of Tween 80 is around 2.5 nm^2,[36] which implies that the chains are densely grafted with a reduced surface coverage of Σ_s/Σ_s^* = 1.5, where Σ_s^* is the surface coverage at overlap and is comparable to the 3D polymer overlap concentration c^*. The shell thickness is estimated to be t = 4 nm, which roughly corresponds to a stretched Tween 80 molecule: 2 nm for the oleate moiety and a bit more than 2 nm for a PEG chain of five units. This is in agreement with the shell thickness of $t = 2 \pm 1$ nm that was previously found from X-ray scattering,[26] where the core−shell contrast predominantly arises from the PEG chains of Tween 80.

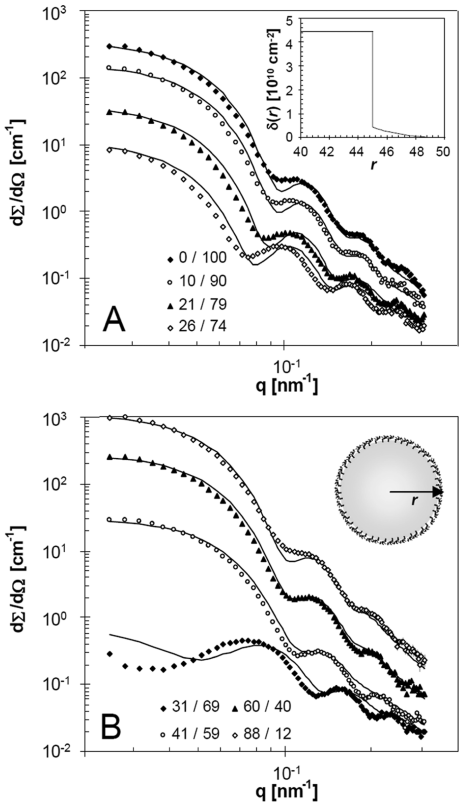

Figure 2. SANS scattering intensities of colloid batch NI2 in eight different H_2O/D_2O mixtures at 20 °C with volume fractions of H_2O/D_2O as given by the legends. Solid lines are model calculations based on the scattering length density profile, $\delta(r)$, shown in the inset of A and discussed in the text and the Supporting Information. The schematic in B depicts the core−shell structure of the colloids.

Charged Colloids. To introduce surface charges onto the Tween 80-coated colloids, we have tested the effect of the addition of a charged comonomer to the emulsion polymerization procedure based on nonionic initiation. We used fully protonated styrene, and the colloids were characterized by dynamic light scattering (DLS). In all cases, we obtained colloids with rather low polydispersity as measured with DLS and listed in Table 2.

The effect of different synthesis conditions (Table 1) on the presence of surface charges was quantified by measurements of the electrophoretic mobility, μ_e. Surprisingly, even for colloid batch NI1, which was synthesized without added anionic comonomer, we found finite values for μ_e of between −0.6 and −2.2 μm·cm/(V·s). The charges causing this are probably introduced by radical-induced degradation of the ester bond that couples the hydrophobic oleate chain of Tween 80 to the hydrophilic PEG headgroup and by the creation of midchain

dx.doi.org/10.1021/la402104q | Langmuir 2013, 29, 11199−11207

Table 2. Characterization of the Synthesized Colloids under Dilute Conditions[a]

		measured in 0.2−20 mM		PB estimates		
colloid batch	R_h (nm)	$-\mu_e$ (μm cm/(V s))	$\lvert Z_{ep}\rvert$	$\lvert Z_{bare}\rvert$	Σ_{bare} (nm^{-2})	$\lvert Z_{sat}\rvert$
NI1	63 ± 8	2.2−0.6	460−780	650	0.013	1260−11 300
NI2	58 ± 9					
MA1	72 ± 10	2.3−0.6	620−950	800	0.012	1440−13 000
MA2	65 ± 15	3.3−0.4	700−980	900	0.017	1300−11 700
MA3	68 ± 13	3.7−0.4	800−1080	1000	0.017	1360−12 200

[a]Hydrodynamic radii (R_h) are determined by DLS. Single-particle electrophoretic mobilities (μ_e) are measured with the Zetasizer for c_s values between 0.2 and 20 mM NaCl/NaN_3 and are used to deduce the surface charge (Z_{ep}) (eqs 1−3, symbols in Figure 3). The bare surface charge (Z_{bare}, eqs 4 and 5), the related bare surface charge density (Σ_{bare}), and the saturated effective surface charge (Z_{sat}, eq 6) for $\kappa_s R$ = 2 and 30 have been estimated from PB charge renormalization theory and should be taken as approximate only.[38]

radicals and subsequent oxidation of the PEG chains themselves.[26,37]

The addition of charged comonomer seems to increase the absolute value of the mobility, as shown in Table 2 for colloid batches MA1−MA3. To quantify this effect further, the electrophoretic effective particle charge number, Z_{ep} (eq 3), is depicted as a function of $\kappa_s R_h$ in Figure 3, where κ_s is the

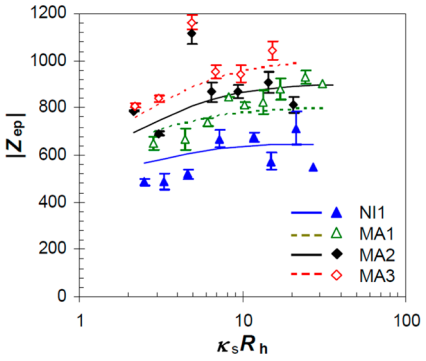

Figure 3. Salt-concentration dependence of the electrophoretic effective charge number, Z_{ep}, of dilute suspensions. Symbols correspond to different colloid batches as listed in the legend. Lines are calculations of $Z_{eff,PB}$ using PB charge renormalization theory as explained in the text.[38]

screening parameter resulting from the salt ions. For all colloid batches, we observe a slight increase in Z_{ep} with increasing $\kappa_s R_h$ values. Qualitatively, this behavior can be explained by the salt-dependent contribution of the counter ions and co-ions to the effective colloid charge and is referred to as charge renormalization.[39] In this context, Z_{ep} can be approximately identified with the effective (renormalized) particle charge number, $Z_{eff,PB}$, as predicted by Poisson−Boltzmann (PB) mean-field theory for an infinitely dilute suspension of spherical particles with monovalent microions.[32] Because $\kappa_s R_h > 2$ in all measurements, we employ the PB-based analytic expression by Aubouy et al.[38] to relate the effective charge number, $Z_{eff,PB}$, to the bare charge number, Z_{bare}, and the added salt concentration[38]

$$|Z_{eff,PB}| = \frac{R}{l_B}\left(4\kappa_s R d + 2d\left(5 - \frac{d^4+3}{d^2+1}\right)\right) \quad (4)$$

with

$$d = D\left(\frac{|Z_{bare}| l_B}{R(2\kappa_s R + 2)}\right) \text{ and } D(x) = \frac{\sqrt{1+x^2}-1}{x} \quad (5)$$

The saturation value of the effective charge number, Z_{sat}, follows from eq 4 by taking the formal limit $Z_{bare} \to \infty$, giving[38]

$$\frac{l_B}{R} Z_{sat} = 4\kappa_s R + 6 + O\left(\frac{1}{\kappa_s R}\right) \quad (6)$$

The lines in Figure 3 are calculated values for $|Z_{eff,PB}|$ using eq 4 and assuming constant values of Z_{bare} (i.e., independent of salinity) as listed in Table 2. The calculated lines follow the trends in the measured Z_{ep} values remarkably well. Table 2 also includes values for Z_{sat}, estimated using eq 6 for the lowest and largest considered salt concentrations. All measured effective charges are well below the estimated saturation values, $|Z_{ep}| < |Z_{sat}|$. These observations suggest that there is significant charge renormalization in the studied salt concentration range and that it cannot be described by relations deduced for the limit of saturated charges. We emphasize that the present analysis does not lead to an accurate determination of the bare surface charge, in particular because possible chemical charge-regulation effects have been ignored. It is rather meant as a qualitative tool to rationalize the observed trends in the effective particle charge as a function of salt concentration and to compare the different colloid batches.

To adjust for the different average radii of the colloid batches, we consider the average bare surface charge density, Σ_{bare}, obtained from dividing Z_{bare} by the surface of a sphere of radius R_h (Table 2). If we also account for the effect of size polydispersity, the spread in Σ_{bare} is on the order of ±0.001 nm^{-2} only. This means that the surface charge density of colloid batch MA1 is not significantly different from that of NI1, whereas the Σ_{bare} values for MA2 and MA3 are significantly larger. We can therefore conclude that the addition of a critical amount of methacrylic acid to the synthesis mixture can effectively increase the surface charge density of the sterically stabilized colloids.

We have noted above that the charges on the colloids from batch NI1 might originate from the cleavage of Tween 80 chains on the surface. To verify that this does not significantly reduce the number of grafted Tween 80 chains and thus the SANS contrast variation results, we compare the grafting densities of Tween 80, Σ_s, to the bare surface charge density, Σ_{bare}. Note that Σ_{bare} is estimated from using the zeta potential, which is defined as the electrostatic potential in the plane of zero shear (i.e., at the outer end of the steric layer). When we recalculate the Tween 80 grafting density in the plane of shear rather than at the core−shell interface, we obtain Σ_s = 0.52 nm^{-2}. This implies that less than 4% of the chains might be cleaved, which would not significantly affect the fitted curves in Figure 2.

dx.doi.org/10.1021/la402104q | Langmuir 2013, 29, 11199−11207

Interacting Colloids. Because the polymeric shell is rather thin compared to the colloid radius, the mutual interactions of the colloids are expected to approach those of perfect hard spheres when the surface charges are fully screened by added salt.[24] With decreasing salt concentrations, the colloidal interactions will be increasingly dominated by screened Coulomb repulsions. To quantify these effects through a colloid−colloid pair potential, we have conducted a series of small-angle X-ray scattering (SAXS) measurements on colloid batches MA2 and MA3 and small-angle neutron scattering (SANS) measurements on colloid batch MA3, focusing on interacting colloids in concentrated suspensions.

First, the efficiency of the steric stabilization at higher colloid concentrations was verified by comparing the SANS data of colloid batch MA3 at $c = 10^2$ g/L in 50 mM and 0.5 M NaCl/NaN_3, as shown in Figure 4. The perfect overlap of the two

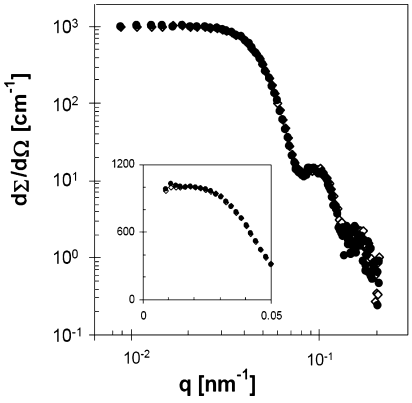

Figure 4. SANS scattering intensities for colloid batch MA3 with $c = 10^2$ g/L in an 84/16 H_2O/D_2O solvent mixture at 20 °C in (●) 50 mM and (◊) 0.5 M NaCl/NaN_3. Inset: close-up view of the low-q data on a double linear scale.

curves indicates the absence of any aggregation or additional attractions at high salt concentrations, which confirms the efficiency of the steric layer in stabilizing the particles.

For colloid batch MA2, a larger series was studied where the colloid concentration was varied between 10^2 and 4×10^2 g/L dispersed in 1.5, 3, 8, 20, or 50 mM NaCl/NaN_3 solutions. The resulting scattering intensities measured by SAXS, $I(q)$, are shown in Figure 5. It is directly apparent that increasing colloid and decreasing salt concentrations enhance the colloidal pair structure: The forward scattering at low-q values steadily decreases, and a clearly observable structure factor principal peak develops at intermediate q values, which becomes more pronounced and moves to higher q values as the colloid concentration is increased. At higher q values, up to five form factor oscillations are visible. This indicates a rather low size polydispersity, s, of the colloids, in line with the value $s = 0.08$ found in our modeling of the SANS contrast variation study (Figure 2).

To distinguish between the particle form factor and the pair-structure contribution to the overall scattering intensity, we use $I(q) \propto cP(q)S(q)$, where $P(q)$ is the average form factor and $S(q)$ is the measurable static structure factor. We have used an iterative approach to extract the SAXS form factor (solid line in Figure 5) and to simultaneously model the structure factors for the whole concentration series, as described in detail in the Supporting Information. The experimental results for the measurable static structure factors are depicted as symbols in

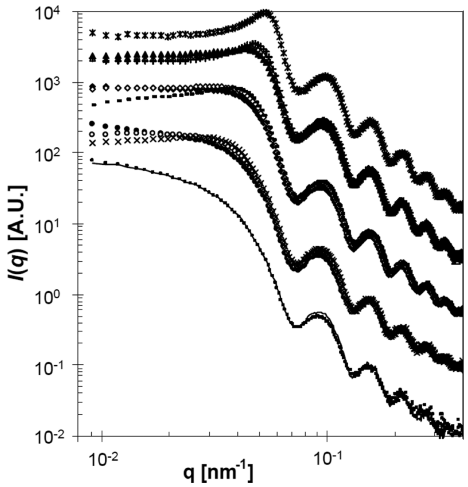

Figure 5. SAXS scattering intensities of colloid batch MA2 in H_2O at 20 °C. From top to bottom, the data correspond to colloid concentrations of $c = 406$, 3×10^2, 2×10^2, 10^2, and 19 g/L. Solid symbols are for 50 mM, open symbols are for 8 mM, asterisk/plus signs are for 3 mM, and cross/minus signs are for 1.5 mM NaCl/NaN_3 solutions. The solid line is the SAXS form factor, which is used to determine the structure factors (details in Supporting Information). For clarity, the data for colloid concentrations $c = 2 \times 10^2$, 3×10^2, and 406 g/L are shifted upward by factors of 5, 5^2, and 5^3, respectively.

Figure 6. The $S(q)$ representation facilitates a comparison with theoretical $S(q)$ calculations, which for a given colloid and salt concentration are determined by the effective pair potential.

Modeling of Structure Factors. We have modeled the measurable static structure factors by employing the semi-analytic MPB-RMSA integral equation scheme for the pair distribution functions of spherical particles in the fluid state interacting via a hard-sphere plus repulsive Yukawa-type effective pair potential.[17] The effect of size polydispersity has been accounted for using the so-called decoupling approximation for the measurable static structure factor. In this approximation, polydispersity in the particles' scattering amplitude is accounted for by calculating the average form factor and measurable static structure factor, whereas all polydispersity in the particle interaction potential is ignored.[8,40]

Comprehensive studies, covering the full (ϕ, κR, Z_{eff}) parameter space in the fluid state, have shown that the MPB-RMSA predictions for the static structure factor are in excellent agreement with results from scattering experiments on suspensions of charged colloidal spheres[17,40] as well as with results from numerically far more expensive Monte Carlo simulations and from the well-established but only numerically solvable Rogers-Young scheme.[17] In the MPB-RMSA calculations, we use the effective pair potential, $U(r)$, in eq 7, which has been shown to describe the equilibrium microstructure of concentrated suspensions properly for the κR values studied here.[41]

$$\beta U(r) = \begin{cases} \infty & \text{for } r \le 2R \\ \dfrac{I_B Z_{eff}^{\ 2} \exp(-\kappa(r-2R))}{r(1+\kappa R)^2} & \text{for } r > 2R \end{cases} \quad (7)$$

Here, β is $1/k_BT$, r is the center-to-center distance of two colloidal spheres of radius R, and κ is an effective inverse screening length that explicitly depends on the colloid volume fraction ϕ. For 1:1 salts, it is given by[17,40,42]

dx.doi.org/10.1021/la402104q | Langmuir 2013, 29, 11199−11207

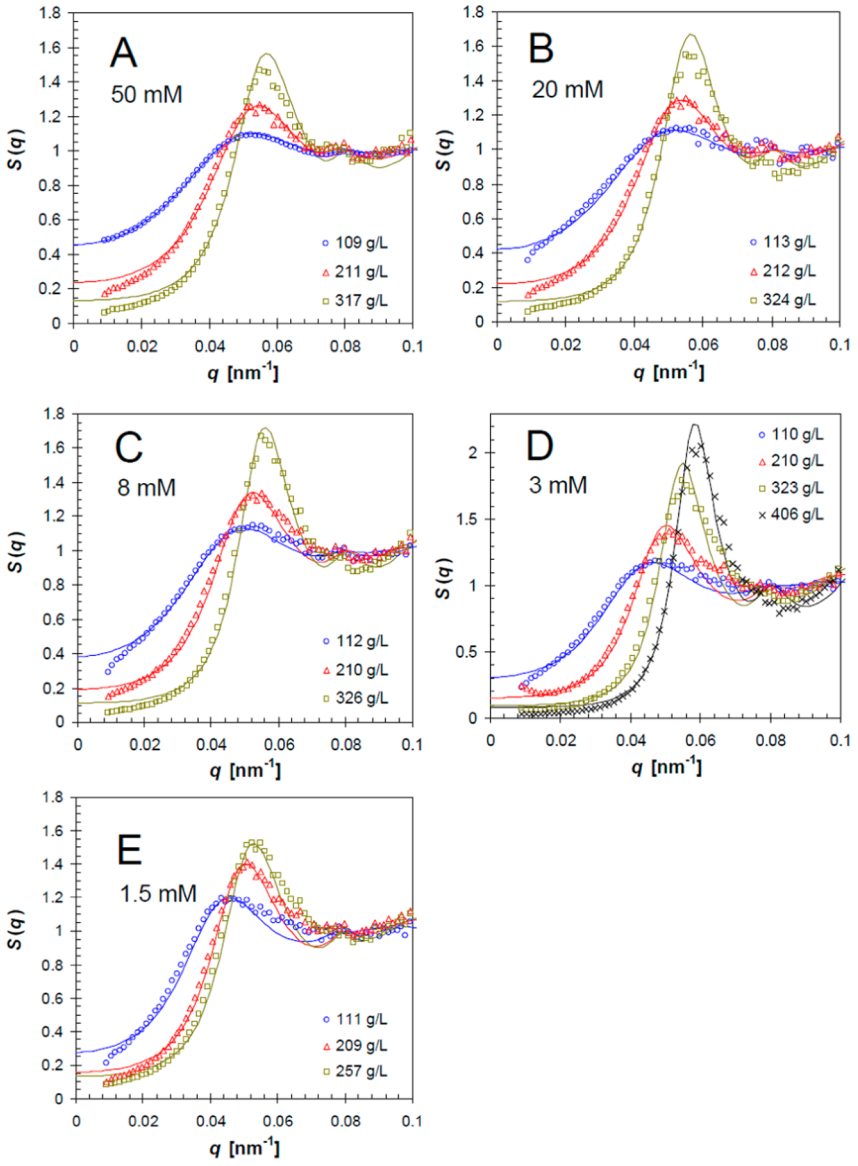

Figure 6. Measurable static structure factors of colloid batch MA2 in H_2O at 20 °C, as deduced from SAXS (symbols). The legends give the colloid concentrations. Added $NaCl/NaN_3$ concentrations are (A) 50, (B) 20, (C) 8, (D) 3, and (E) 1.5 mM. Solid lines are theoretical model calculations for weakly polydisperse spheres interacting via the effective pair potential in eq 7 using the MPB-RMSA scheme[17] in conjunction with the decoupling approximation.[8]

$$\kappa = \left(l_B \left(\frac{3\phi |Z_{eff}|}{R^3(1-\phi)} + 8\pi c_s N_A \right) \right)^{0.5} \quad (8)$$

Here, c_s is the salt concentration in the continuous solvent phase. Equation 7 implicitly assumes that the core−shell particles can be described as hard spheres with an effective hard-sphere volume fraction, ϕ. Extending our earlier discussion of charge renormalization at zero colloid concentration, $Z_{eff}(\phi)$ in eqs 7 and 8 is an effective (renormalized) charge number for a system at nonzero colloid concentration. Since Z_{ep} approaches a constant value for $\kappa_s R > 20$ (Figure 3), also Z_{eff} is assumed to be constant for $\kappa R > 20$. On the basis of the SANS contrast variation results, the size polydispersity is taken as $s = 0.08$. In all, three adjustable parameters have been used in our theoretical modeling of $S(q)$: the particle radius R and the single-particle mass density c/ϕ are assigned a constant value for all considered systems, while Z_{eff} is kept constant for $c_s \geq 20$ mM but allowed to decrease for $c_s \leq 8$ mM (cf. Table 3).

The theoretical results for the measurable static structure factors are depicted in Figure 6 as solid lines, and the corresponding model parameters are listed in Table 3. The theoretical model calculations describe the experimental data set very well over the whole range of colloid and salt concentrations. We find a hard-sphere radius of $R = 55.5$ nm with a precision of ±1 nm using a value of $c/\phi = 1040$ g/L. The effective surface charges obtained from the $S(q)$ modeling (Table 3) are smaller than those found from the electrophoretic mobility measurements for dilute systems (Table 2), corresponding respectively to $Z_{eff} = 500 \pm 50$ and $Z_{ep} = 900 \pm 400$ at $\kappa R > 20$. Even though Z_{ep} and Z_{eff} are not expected to be equal to each other,[43] the observed difference is actually not so large considering the strong dependence of the absolute value of Z_{ep} on the value for R_h (eqs 1−3). In line with the Z_{ep} results, Z_{eff} decreases with decreasing salt concentration for κR

dx.doi.org/10.1021/la402104q | Langmuir 2013, 29, 11199−11207

Table 3. Model Parameters for the SAXS Measurable Static Structure Factors of Colloid Batch MA2, Obtained by Using the MPB-RMSA Plus Decoupling Approximation Scheme for Yukawa-Type Spheres with Mean Radius R = 55.5 ± 1 nm, Size Polydispersity s = 0.08, and c/ϕ = 1040 g/L

dispersion parameters		model parameters		
c_s (mM)	c (g/L)	κR	ϕ	Z_{eff}
50	109	41	0.105	500
50	211	41	0.203	500
50	317	41	0.305	500
20	113	26	0.109	500
20	212	26	0.203	500
20	324	26	0.311	500
8.1	112	16	0.107	500
8.0	210	16	0.202	430
7.8	326	16	0.313	300
3.0	110	10	0.106	500
3.0	210	10	0.202	370
3.0	323	10	0.311	260
3.0	406	10	0.390	170
1.5	111	7.1	0.107	300
1.5	209	7.1	0.201	180
1.5	257	7.2	0.247	180

< 20. Moreover, Z_{eff} shows a significant additional volume fraction dependence.

Although theoretical charge renormalization studies have been extended to higher volume fractions,[41,42,44] they mainly focused on significantly lower screening conditions or higher bare surface charges, where κ is predominantly determined by the counterions released from the colloid surface. Because the surface charges on the present colloids originate from weakly acidic −COOH groups, chemical charge regulation can play a role in addition to charge renormalization.[42] A detailed combined modeling of surface charge regulation and renormalization and the analysis of its effect on $S(q)$ is outside the scope of the present work.[39,41,45]

To confirm the consistency and accuracy of our theoretical modeling of SAXS data, we have additionally characterized a concentration and added salt series of colloid batch MA3 using both SAXS and SANS. The results of this additional analysis are summarized in the Supporting Information. SANS has the advantage over SAXS in that the contrast can be adjusted to minimize the effect of background scattering compared to colloid scattering. The SAXS beamline used in our study allows faster data acquisition with basically no smearing. Because the contrast of the two methods is set by different material properties, they nicely complement each other. Indeed, we find good agreement between the results by SANS and SAXS for colloid batch MA3. The mean colloid radius is R = 62 ± 2 nm, and the effective surface charge number is Z_{eff} = 550 ± 50 for κR > 20, which decreases to Z_{eff} = 230 ± 30 for c = 309 g/L and 1.5 mM NaCl/NaN_3. Consistent with the results for colloid batch MA2, colloid batch MA3 shows charge renormalization as a function of both salt and colloid concentrations.

CONCLUSIONS

We have synthesized and characterized aqueous dispersions of polystyrene colloids that behave as effective hard spheres at very high salt concentrations and show electrostatic repulsions at lower salt content that can be tuned (i.e., continuously enlarged) by a further decrease in the salt concentration. A grafted surfactant layer of 4 nm thickness effectively screens the van der Waals attractions between the cores to such an extent that even the addition of salt up to 0.5 M does not lead to any signature of attraction between the colloids. The surface charge density can be adjusted by the addition of a critical amount of charged comonomer during the synthesis procedure. Under dilute colloid conditions, the electrophoretic effective surface charge tends to decrease with decreasing salt concentration, which can be qualitatively explained by an easy-to-apply analytical expression derived from PB theory for larger $\kappa_s R$ values and is applicable to effective surface charges below saturation.[38]

We have analyzed the equilibrium microstructure of the colloids over a wide range of colloid and salt concentrations using SAXS and SANS. By applying the MPB-RMSA plus decoupling approximation scheme using a Yukawa-type plus excluded volume repulsive pair potential,[17] we could consistently reproduce the overall shape of the experimentally deduced measurable static structure factor for all considered colloid concentrations and salinities. Both the salt and colloid concentration dependences of the effective particle charge Z_{eff} have been studied, which are significantly affected by charge renormalization. A more detailed analysis of the complicated relation between effective and bare charges is outside the scope of this work. Such an analysis will require detailed charge renormalization calculations including a realistic modeling of the chemical charge regulation of the core−shell particles.[42]

So far, experimental studies of $S(q)$ with an accompanying theoretical investigation of effective particle charges were mostly concerned with low-salinity colloidal systems or colloids with high intrinsic surface charges.[13,42] One important reason for us to develop this model system was to establish a well-defined aqueous colloidal system with not too strong electrostatic repulsions at intermediate salt concentrations that can be easily tuned and remain stable even at high salt content. Our experimental and theoretical results underline the relevance of a careful characterization of the repulsions in the full (c_s, ϕ) phase space. The characterization achieved in this work is expected to be useful in future studies of crystal, glass, and gel states of the presented model system at high concentrations.

ASSOCIATED CONTENT

Supporting Information

Core−shell model for the contrast variation study of colloid batch NI2. Determination of SAXS structure factors for colloid batch MA2. SANS and SAXS scattering intensities for colloid batch MA3 as a function of colloid and salt concentrations, including MPB-RMSA calculations of the SANS and SAXS structure factors. This material is available free of charge via the Internet at http://pubs.acs.org.

AUTHOR INFORMATION

Corresponding Author

*E-mail: anna.stradner@fkem1.lu.se. Tel: +46-46-2228214.

Notes

The authors declare no competing financial interest.

ACKNOWLEDGMENTS

K.v.G. and A.S. gratefully acknowledge financial support from the Swiss National Science Foundation (SNF, 200021_119964), the University of Fribourg, and the Adolphe

Merkle Foundation. M.H. acknowledges funding by the European Research Council (ERC) Advanced Grant INTERCOCOS, FP7 ref. no. 267499. The SAXS experiments were financially supported by the European Commission under the Seventh Framework Program by means of the grant agreement for Integrated Infrastructure Initiative no. 262348 European Soft Matter Infrastructure (ESMI). We thank Shirish Chodankar and Andreas Menzel for their help as local contacts for the SAXS measurements and Joachim Kohlbrecher for the SANS measurements. We thank Liliane Ackermann-Hirschi for her help with the syntheses.

REFERENCES

(1) Russel, W. B. *Colloidal Dispersions*; Cambridge University Press: New York, 1989.
(2) Belloni, L. Colloidal interactions. *J. Phys.: Condens. Matter* **2000**, *12*, R549−R587.
(3) Hidalgo-Alvarez, R.; Martin, A.; Fernandez, A.; Bastos, D.; Martinez, F.; De las Nieves, F. J. Electrokinetic properties, colloidal stability and aggregation kinetics of polymer colloids. *Adv. Colloid Interface Sci.* **1996**, *67*, 1−118.
(4) Levin, Y. Electrostatic correlations: from plasma to biology. *Rep. Prog. Phys.* **2002**, *65*, 1577−1632.
(5) John, S. Strong localization of photons in certain disordered dielectric superlattices. *Phys. Rev. Lett.* **1987**, *58*, 2486−2489.
(6) Pan, G. S.; Kesavamoorthy, R.; Asher, S. A. Optically nonlinear Bragg diffracting nanosecond optical switches. *Phys. Rev. Lett.* **1997**, *78*, 3860−3863.
(7) Yablonovitch, E. Inhibited spontaneous emission in solid-state physics and electronics. *Phys. Rev. Lett.* **1987**, *58*, 2059−2062.
(8) Nägele, G. On the dynamics and structure of charge-stabilized suspensions. *Phys. Rep.* **1996**, *272*, 216−372.
(9) Beck, C.; Härtl, W.; Hempelmann, R. The glass transition of charged and hard sphere silica colloids. *J. Chem. Phys.* **1999**, *111*, 8209−8213.
(10) Derjaguin, B.; Landau, L. Theory of stability of highly charged liophobic sols and adhesion of highly charged particles in solutions of electrolytes. *Zh. Eksp. Teor. Fiz.* **1945**, *15*, 663−682.
(11) Verwey, E. J. W.; Overbeek, J. T. G. *Theory of Stability of Lyophobic Colloids*; Elsevier: Amsterdam, 1948.
(12) Behrens, S. H.; Christl, D. I.; Emmerzael, R.; Schurtenberger, P.; Borkovec, M. Charging and aggregation properties of carboxyl latex particles: experiments versus DLVO theory. *Langmuir* **2000**, *16*, 2566−2575.
(13) Quesada-Perez, M.; Callejas-Fernandez, J.; Hidalgo-Alvarez, R. Interaction potentials, structural ordering and effective charges in dispersions of charged colloidal particles. *Adv. Colloid Interface Sci.* **2002**, *95*, 295−315.
(14) Hamaker, H. C. The London-van der Waals attraction between spherical particles. *Physica* **1937**, *4*, 1058−1072.
(15) Lifshitz, E. M. The theory of molecular attractive forces between solids. *Sov. Phys. JETP* **1956**, *2*, 73−83.
(16) Philipse, A. P.; Vrij, A. Determination of static and dynamic interactions between monodisperse, charged silica spheres in an optically matching, organic-solvent. *J. Chem. Phys.* **1988**, *88*, 6459−6470.
(17) Heinen, M.; Holmqvist, P.; Banchio, A. J.; Nägele, G. Pair structure of the hard-sphere Yukawa fluid: an improved analytic method versus simulations, Rogers-Young scheme, and experiment. *J. Chem. Phys.* **2011**, *134*, 044532. Heinen, M.; Holmqvist, P.; Banchio, A. J.; Nägele, G. Errarum: "Pair structure of the hard-sphere Yukawa fluid: an improved analytic method versus simulations, Rogers-Young scheme, and experiment". *J. Chem. Phys.* **2011**, *134*, 129901.
(18) Holmqvist, P.; Nägele, G. Long-time dynamics of concentrated charge-stabilized colloids. *Phys. Rev. Lett.* **2010**, *104*, 058301.
(19) Degiorgio, V.; Piazza, R.; Bellini, T.; Visca, M. Static and dynamic light-scattering study of fluorinated polymer colloids with a crystalline internal structure. *Adv. Colloid Interface Sci.* **1994**, *48*, 61−91.
(20) Pusey, P. N.; Van Megen, W. Phase-behavior of concentrated suspensions of nearly hard colloidal spheres. *Nature* **1986**, *320*, 340−342.
(21) Hartenstein, M.; Weiss, A.; Seelenmeyer, S.; Ballauff, M. Adsorption of anions on the surface of charge-free latex particles as revealed by turbidimetric measurements. *J. Colloid Interface Sci.* **1998**, *208*, 266−271.
(22) Zackrisson, M.; Stradner, A.; Schurtenberger, P.; Bergenholtz, J. Small-angle neutron scattering on a core-shell colloidal system: a contrast-variation study. *Langmuir* **2005**, *21*, 10835−10845.
(23) Zackrisson, M.; Stradner, A.; Schurtenberger, P.; Bergenholtz, J. Structure, dynamics, and rheology of concentrated dispersions of poly(ethylene glycol)-grafted colloids. *Phys. Rev. E* **2006**, *73*, 011408.
(24) Royall, C. P.; Poon, W. C. K.; Weeks, E. R. In search of colloidal hard spheres. *Soft Matter* **2013**, *9*, 17−27.
(25) Fortini, A.; Dijkstra, M.; Tuinier, R. Phase behaviour of charged colloidal sphere dispersions with added polymer chains. *J. Phys.: Condens. Matter* **2005**, *17*, 7783−7803.
(26) Weiss, A.; Hartenstein, M.; Dingenouts, N.; Ballauff, M. Preparation and characterization of well defined sterically stabilized latex particles with narrow size distribution. *Colloid Polym. Sci.* **1998**, *276*, 794−799.
(27) Slawinski, M.; Meuldijk, J.; Van Herk, A. M.; German, A. L. Seeded emulsion polymerization of styrene: incorporation of acrylic acid in latex products. *J. Appl. Polym. Sci.* **2000**, *78*, 875−885.
(28) Van Gruijthuijsen, K.; Rufier, C.; Phou, T.; Obiols-Rabasa, M.; Stradner, A. Light and neutron scattering study of PEG-oleate and its use in emulsion polymerization. *Langmuir* **2012**, *28*, 10381−10388.
(29) Brown, J. C.; Pusey, P. N. Measurement of diffusion-coefficients of polydisperse solutes by photon correlation spectroscopy. *J. Phys D: Appl. Phys.* **1974**, *7*, L31−L35.
(30) Koppel, D. E. Analysis of macromolecular polydispersity in intensity correlation spectroscopy - method of cumulants. *J. Chem. Phys.* **1972**, *57*, 4814−4820.
(31) Ohshima, H. *Theory of Colloid and Interfacial Electric Phenomena*; Elsevier Academic Press: New York, 2006.
(32) Palberg, T.; Monch, W.; Bitzer, F.; Piazza, R.; Bellini, T. Freezing transition for colloids with adjustable charge - A test of charge renormalization. *Phys. Rev. Lett.* **1995**, *74*, 4555−4558.
(33) Gapinski, J.; Patkowski, A.; Banchio, A. J.; Buitenhuis, J.; Holmqvist, P.; Lettinga, M. P.; Meier, G.; Nägele, G. Structure and short-time dynamics in suspensions of charged silica spheres in the entire fluid regime. *J. Chem. Phys.* **2009**, *130*, 084503.
(34) Keiderling, U. *"BerSANS" Data Reduction Program*; HMI Berlin: Berlin, 1994−2008.
(35) Lindner, P.; Zemb, T. *Neutrons, X-rays and Light: Scattering Methods Applied to Soft Condensed Matter*; Elsevier Science B.V.: Amsterdam, 2002.
(36) Haque, M. E.; Das, A. R.; Moulik, S. P. Mixed micelles of sodium deoxycholate and polyoxyethylene sorbitan monooleate (Tween 80). *J. Colloid Interface Sci.* **1999**, *217*, 1−7.
(37) Thickett, S. C.; Gilbert, R. G. Emulsion polymerization: state of the art in kinetics and mechanisms. *Polymer* **2007**, *48*, 6965−6991.
(38) Aubouy, M.; Trizac, E.; Bocquet, L. Effective charge versus bare charge: an analytical estimate for colloids in the infinite dilution limit. *J. Phys. A* **2003**, *36*, 5835−5840.
(39) Alexander, S.; Chaikin, P. M.; Grant, P.; Morales, G. J.; Pincus, P.; Hone, D. Charge renormalization, osmotic-pressure, and bulk modulus of colloidal crystals - theory. *J. Chem. Phys.* **1984**, *80*, 5776−5781.
(40) Westermeier, F.; Fischer, B.; Roseker, W.; Grübel, G.; Nägele, G.; Heinen, M. Structure and short-time dynamics in concentrated suspensions of charged colloids. *J. Chem. Phys.* **2012**, *137*, 114505.
(41) Dobnikar, J.; Castaneda-Priego, R.; Von Grünberg, H. H.; Trizac, E. Testing the relevance of effective interaction potentials between highly-charged colloids in suspension. *New J. Phys.* **2006**, *8*, 277.

(42) Gisler, T.; Schulz, S. F.; Borkovec, M.; Sticher, H.; Schurtenberger, P.; D'Aguanno, B.; Klein, R. Understanding colloidal charge renormalization from surface-chemistry - experiment and theory. *J. Chem. Phys.* **1994**, *101*, 9924−9936.
(43) Wagner, N. J.; Krause, R.; Rennie, A. R.; D'Aguanno, B.; Goodwin, J. The microstructure of polydisperse, charged colloidal suspensions by light and neutron-scattering. *J. Chem. Phys.* **1991**, *95*, 494−508.
(44) Trizac, E.; Aubouy, M.; Bocquet, L. Analytical estimation of effective charges at saturation in Poisson-Boltzmann cell models. *J. Phys.: Condens. Matter* **2003**, *15*, S291−S296.
(45) Colla, T. E.; Levin, Y.; Trizac, E. A self-consistent renormalized jellium approach for calculating structural and thermodynamic properties of charge stabilized colloidal suspensions. *J. Chem. Phys.* **2009**, *131*, 074115.